



*J. Serb. Chem. Soc.* 82 (7–8) 851–864 (2017)  
JSCS–5007

## Solvent, substituents and pH effects towards the spectral shifts of some highly coloured indicators

MAMDOUH S. MASOUD, REHAB M. I. ELSAMRA\* and SOKAINA S. HEMDAN

*Department of Chemistry, Faculty of Science, Alexandria University, Alexandria, Egypt*

(Received 4 February, accepted 2 March 2017)

**Abstract:** The solvatochromic responses of six indicators namely Sudan orange, Alizarin yellow R, Aurin tricarboxylic acid, Alizarin yellow GG, Titan yellow and Eriochrome black-T, dissolved in seven solvents of different polarities, have been measured at room temperature. The UV/Vis absorption spectral shifts were analyzed by the multiple linear regression analysis and Kamlet–Taft equation. The observed solvatochromism was found to depend on the presence of the donor and acceptor substituents in the conjugated systems of the indicator and the physical properties of the solvent molecules. The pH effects on the wavenumbers of the absorption band maxima of some indicators with different constituents at room temperature were discussed and the mechanism of ionization was explained. The dissociation constants ( $pK_a$ ) of the investigated compounds were precisely assessed and the existence of the individual predominant ionic species was assigned by constructing distribution diagrams at different pH ranges.

**Keywords:** azo dyes; solvatochromism; Kamlet–Taft parameters; acid dissociation constant.

### INTRODUCTION

Indicators are widely used in analytical chemistry for quantitative and qualitative analysis.<sup>1</sup> Most indicators possess an azo group conjugated to one or two arenes. The presence of donor and acceptor substituents in the conjugated systems of the indicator can be of interest in the study of solvent and substituent effects on the UV/Vis spectroscopic absorption maxima,  $\lambda_{max}$ , of the azobenzene dyes. Also, the planarity of the azo group is in contrast with the other part of the system, and it should allow larger  $\pi$  electron transmission and lead to higher optical activity.<sup>2</sup> The application of the techniques of multiple linear regression has proved to be significantly successful and has greatly improved the understanding of the solvent role.<sup>3</sup> Besides, the dissociation constant ( $pK_a$ ) is an imp-

\* Corresponding author. E-mail: rehab\_elsamra@hotmail.com  
doi: 10.2298/JSC170204032M

important physicochemical parameter in the biophysical characterization of using azo dyes as drugs and may be helpful in predicting the behaviour of a drug under *in vivo* conditions.<sup>4</sup>

This article is part of a continuing investigation of the structural chemistry of biologically active compounds containing nitroso, nitro and azo chromophoric groups.<sup>5–11</sup> Here, we aimed to throw light on the solvents effect on the absorption spectra of highly coloured indicators (Sudan orange (SO), Alizarin yellow R (AYR), Aurin tricarboxylic acid (ATA), Alizarin yellow GG (AYGG), Titan yellow (TY) and Eriochrome black-T (EBT)) in the visible and UV region where these compounds absorb due to the extensive conjugation of the azo group with the aromatic rings. Solvents are selected to show a wide variety of solvent parameters and hydrogen bonding capacity, to permit a good understanding of the solvent-induced spectral shifts. Moreover, the UV–Vis absorption spectra of some indicators were investigated in aqueous buffer solutions of different pH values and used for computing the dissociation constants ( $pK_a$ ). The ranges of pH, where individual ionic species are predominant have been determined.

## EXPERIMENTAL

### *Chemicals and materials*

All indicators and starting materials used in this work were purchased from Fluka, BDH and Sigma companies. The chemical structures of the investigated indicators and their abbreviations are presented in Fig. S-1 of the Supplementary material to this paper. The solvents were of HPLC grade and have been used without further purification. All solutions were prepared with de-ionized and CO<sub>2</sub>-free water. The universal buffer used in this study was prepared by mixing 0.04 M of H<sub>3</sub>BO<sub>3</sub>, H<sub>3</sub>PO<sub>4</sub> and CH<sub>3</sub>COOH acids and adding the required volume of 0.2 M KOH (CO<sub>2</sub> free) to give the desired pH. The ionic strength of the studied solution was adjusted by adding 0.5 M solution of KCl.

### *Procedure*

UV/Vis absorption spectral measurements were recorded for each indicator in the proper solvent with a Perkin-Elmer Lambda 19 spectrophotometer model cell, covering the wavelength range 200–900 nm at room temperature (~20 °C). Seven different solvents namely 1,4-dioxane, ethanol (EtOH), *N,N*-dimethylformamide (DMF), dimethyl sulfoxide (DMSO), acetone, acetonitrile and water were used. These solvents have different polarity parameters ( $E$ ,  $K$ ,  $M$ ,  $J$ ,  $H$  and  $N$ ), mainly related to the refractive index  $n$  and dielectric constant  $D^*$  of each solvent.<sup>12–15</sup> The solvatochromic parameters ( $\pi^*$ ,  $\alpha$  and  $\beta$ ) were taken from literature.<sup>16</sup> The physical parameters for the solvents at 20 °C are collected in Table S-I of the Supplementary material. The dissociation constants of the indicators were determined by means of the data obtained in the pH range 3.0–11.5. The pH value was measured by using previously calibrated Martini instrument pH-benchmeter.

### *Data treatment*

The observed peak position of an absorption band,  $Y$ , in a given solvent has been expressed as a linear function using different combinations (one-, two-, three- and four) of solvent polarity parameters ( $E$ ,  $K$ ,  $M$ ,  $J$ ,  $H$  and  $N$ ),  $X_n$ , by:

\* Relative permittivity,  $\epsilon_r$

$$Y = a_0 + a_1X_1 + a_2X_2 + \dots + a_nX_n \quad (1)$$

The regression intercept,  $a_0$ , has been assumed to be an estimate of the peak position for the gas phase spectra.  $a_1, a_2, \dots, a_n$  are the solvent polarity parameters coefficients.<sup>17</sup> SPSS program has been used to determine these coefficients by multiple regression technique. The effect of specific chemical interactions (hydrogen bonding) and non-specific solvent interactions (dipolarity/polarizability) on the position of the UV/Vis absorption bands of the studied indicators have been evaluated by using the Kamlet–Taft approach:<sup>18</sup>

$$\nu_{\max} = \nu_{\max,0} + a\alpha + b\beta + s\pi^* \quad (2)$$

where  $\nu_{\max}$  is the maximum wavenumber ( $\text{cm}^{-1}$ ) of the absorption band of the indicator dissolved in pure solvent.  $\nu_{\max,0}$  is the solute property of a reference system and represents the regression intercept which corresponds to the gaseous state of the spectrally active substance.  $\alpha$  describes the HBD (hydrogen-bond donating) ability or solvent “acidity”,  $\beta$  the HBA (hydrogen-bond accepting) ability or solvent “basicity”,  $\pi^*$  the dipolarity/polarizability of the solvents.  $a, b$  and  $s$  are solvent-independent correlation coefficients that indicate the contribution of each solvatochromic parameters to the UV/Vis absorption peak shift.

## RESULTS AND DISCUSSION

### *Solvent effects on the UV–Vis absorption spectra*

The electronic absorption spectra of Sudan orange (SO) in presence of different solvents is selected for demonstration, Fig. 1. Different absorption bands of the investigated indicators in different solvents are listed in Table I. Generally, the electronic absorption spectra of the compounds in solution exhibit two types of bands. The shorter wavelength band in the UV region of 247–326 nm is observed in all solvents used – except in acetone – which is ascribed mainly to the  $\pi$ - $\pi^*$  transition of the aromatic system present in the structure of the studied indicators. The second band observed in the region of 307–540 nm is assigned to  $n$ - $\pi^*$  transition with a considerable charge-transfer character (CT transition). The charge-transfer nature of this band is deduced from its broadness, as from the sensitivity of its  $\lambda_{\max}$  to the type of substituent attached to the azo coupler.<sup>19</sup>

In addition to the lone pair of electrons of the azo group, the arene moiety of the molecules contains different substituents possessing nitrogen, oxygen or sulphur atoms (*e.g.*,  $\text{NO}_2$ ,  $\text{SO}_3\text{H}$ ,  $\text{COOH}$  and  $\text{OH}$  groups). For example, the region 307–370 nm is assigned to  $n$ - $\pi^*$  of  $\text{COOH}$ ,  $\text{OH}$  and  $\text{NO}_2$  groups (*e.g.*, SO, EBT and AYGG). Bands observed at longer wavelength (*e.g.*, at 500 nm in EBT) is attributed to the weak forbidden  $n$ - $\pi^*$  transitions.<sup>20</sup> It was observed that the main bands of the compounds (SO and AYR) which are located in the range of 310–550 nm exhibit an apparent shift towards longer wavelengths in different solvents according to the sequence: 1,4-dioxane < acetone < acetonitrile < EtOH < DMSO <  $\text{H}_2\text{O}$ . This shift is in agreement with the change in the polarity of the organic solvents and could be considered as a result of the combination of the several solvent characteristics such as polarity and hydrogen bonding. Furthermore, the electronic spectra of the compound ATA in DMF and DMSO contains

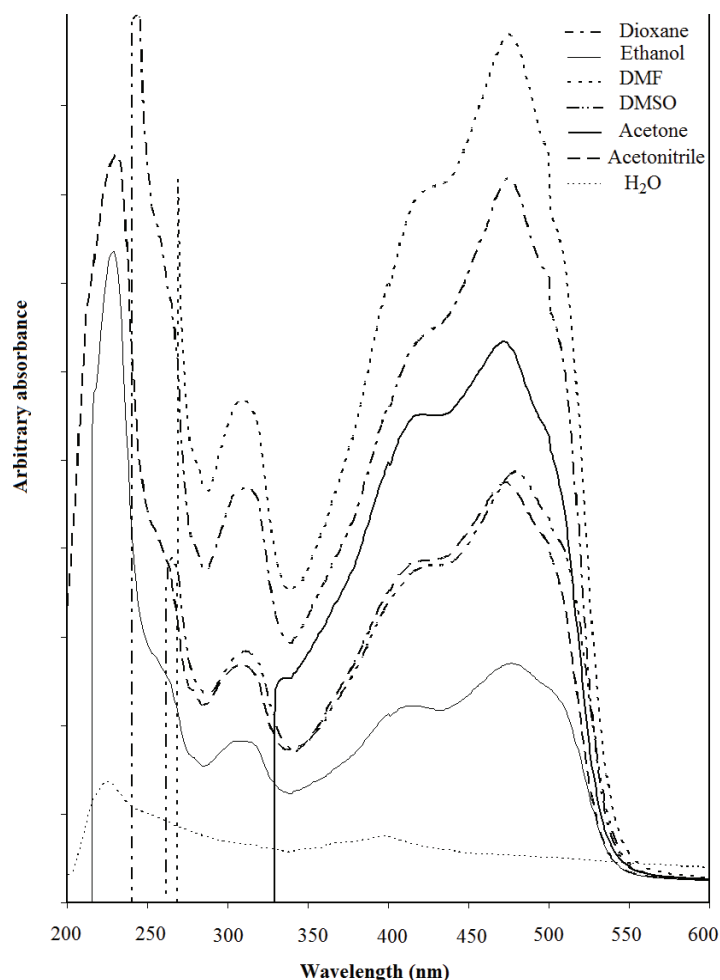


Fig. 1. Electronic absorption spectra of Sudan orange in the presence of different solvents.

a new band appearing at much longer wavelength at 544 and 561 nm, respectively, Table I, owing to solvated complex formation between solute molecules with DMF and DMSO molecules through an intermolecular H-bonding.<sup>21</sup> Moreover, the  $\pi$ - $\pi^*$  band is red shifted when proceeding from the nonpolar solvent 1,4-dioxane (e.g., AYR:  $\lambda_{\max} = 290$  nm) to polar solvent H<sub>2</sub>O ( $\lambda_{\max} = 301$  nm). This red shift is mainly due to  $\pi^*$  orbital stabilization in polar solvents more than the  $\pi$  orbital. All the studied indicators, except ATA, possess an azo group conjugated with two arenes. The *trans* azo isomer possesses a lower steric hindrance compared to the *cis* isomer with possible azo-hydrazone tautomerism.<sup>22</sup> The following intramolecularly hydrogen-bonded structures are expected to be the most stable, e.g., SO (Fig. 2).

TABLE I. Electronic absorption spectra of the indicators in presence of different solvents ( $\lambda_{\max}$  / nm)

Compound	1,4-Dioxane	Ethanol	DMF	DMSO	Acetone	Acetonitrile	H <sub>2</sub> O
EBT	287	281	274	284	–	286	278
	379	–	330	331	366	332	338
	403	394	399	398	403	400	–
	500	509	–	513	500	504	535
SO	265	259	269	266	–	260	–
	312	307	309	312	–	309	–
	414	408	424	425	412	407	395
	470	477	475	497	468	473	508
AYR	–	271	281	270	–	235	236
	290	296	308	306	–	305	301
	386	392	392	391	389	400	395
	–	–	540	–	542	–	–
ATA	–	247	–	262	–	234	239
	290	301	311	304	–	306	303
	395	392	393	398	396	400	388
	–	–	544	561	–	–	–
AYGG	262	260	270	263	–	257	259
	365	364	346	350	347	370	353
	–	–	393	–	384	–	–
TY	–	326	322	322	–	318	320
	–	412	412	418	400	400	408
	–	–	–	–	–	–	–



Fig. 2. Azo-hydrazone tautomerism of Sudan orange.

### Regression analysis

Regression analysis data for  $Y_1$  and  $Y_2$  bands ( $Y_1$ :  $\lambda_{\max}$  ~ 257 to 326 nm and  $Y_2$ :  $\lambda_{\max}$  from 346 to 425 nm) of the investigated indicators is given in Tables S-II–S-VII of the Supplementary material. A value of multiple correlation coefficient ( $MCC$ ) near to unity and/or a small value (near zero) of the significance parameter ( $P$ ) mean the correlation is good. The analysis of the spectral shifts using one-parameter equation showed that all  $MCC$  values for all solvent parameters are very poor, indicating the difficulty of correlation for the studied spectral region  $Y_1$  and  $Y_2$ . However, the parameter  $K$  gives a moderate correlation ( $MCC = 0.767, 0.640$  and  $0.423$  for ATA, AYR and TY, respectively) for the region  $Y_1$ , *i.e.*, the dielectric constant ( $D$ ) of the solvent is the predominant parameter to explain the spectral shifts. The regression analysis of the two-parameter equations improves the correlations. For instance, when the parameter  $E$  is com-

bined with the parameter  $M$ , e.g., SO, the  $MCC$  value jumped from 0.585 to 0.816 for the region  $Y_2$ , Table S-II. This is probably due to the presence of the OH substituent in the ortho position of the arylazo moiety which eases the formation of hydrogen bonds with the solvent.

For the studied spectral region  $Y_1$ , the three-combinations ( $K,M,E$ ), ( $K,N,E$ ) and ( $M,N,E$ ) for TY ( $\text{SO}_3\text{H}$  and  $\text{CH}_3$  substituents), Table S-VII, shows better fit when compared to ATA ( $\text{COOH}$  and OH substituents), Table S-IV. Also, the combinations ( $K,M,E$ ), ( $K,N,E$ ) and ( $M,N,E$ ) for AYGG ( $m\text{-NO}_2$ ), Table S-V, show poor fit when compared to AYR ( $p\text{-NO}_2$ ), Table S-III. The four parameters combinations for all compounds showed the best fit of a value of  $MCC$ , which equals nearly 1.000. This leads to the assumption that the combination of different solvent parameters  $K$ ,  $M$ ,  $N$  and  $E$  is effective to explain the spectral shifts depending on the electronic character of the substituent and the position of this substituent in the arene moiety of the studied indicators.

#### *Kamlet and Taft method*

The results of the correlation of the absorption frequencies with the Kamlet–Taft solvatochromic parameters  $\pi^*$ ,  $\alpha$  and  $\beta$  using SPSS program are given in Table II, where the values of  $R$  (correlation coefficient) showing the quality of the multiparametric correlation. Figure 3 shows the relationship between the absorption maxima ( $\nu_{\text{max}}$  (calculated)) predicted by the multicomponent linear regression using the estimated  $\nu_{\text{max},0}$ ,  $a$ ,  $b$  and  $s$  coefficients against the experimental values ( $\nu_{\text{max}}$  (measured)) for SO as a representative example.

TABLE II. Results of the Kamlet and Taft correlation model for all indicators

Indicator	$s / 10^3 \text{ cm}^{-1}$	$a / 10^3 \text{ cm}^{-1}$	$b / 10^3 \text{ cm}^{-1}$	$\nu_{\text{max},0} / 10^3 \text{ cm}^{-1}$	$R$
EBT	0.532	0.600	0.288	24.369	0.959
SO	-0.129	1.135	-1.744	24.969	0.992
AYR	-0.466	-0.180	0.419	25.698	0.537
ATA	0.056	0.401	0.222	25.050	0.784
AYGG	2.068	-0.499	1.573	25.742	0.741
TY	-0.829	-0.048	-2.120	26.430	0.967

There is a linear relationship for all samples, Fig. 3, indicating the high correlation obtained by multilinear regression according to Kamlet–Taft equation. Also, the correlation coefficients,  $R$ , are nearly of the same magnitude for all indicators, showing the high quality of the multiparametric equation (Table II). The negative sign of  $b$  coefficient for the indicators TY and SO shows a positive solvatochromism or bathochromic shifts of these compounds with increasing the solvent HBA “solvent basicity”. The positive sign of both  $s$  and  $a$  coefficients for the indicators EBT and ATA points to the hypsochromic shifts of the studied compounds with increasing of solvent dipolarity/polarizability and solvent HBD

“solvent acidity”. The percentage contribution of the calculated solvatochromic parameters from the values of regression coefficients are given in Table III and Fig. 4.

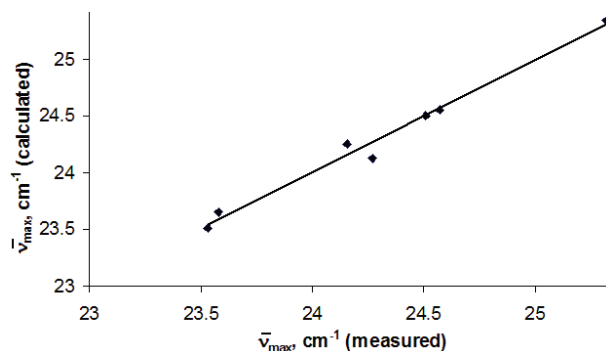


Fig. 3. Linear relationship between the experimental and the calculated absorption maxima ( $\nu_{\max} \times 10^{-3} \text{ cm}^{-1}$ ) of SO indicator obtained by multilinear regression according to Kamlet–Taft equation.

TABLE III. Percentage contribution of calculated solvatochromic parameters,  $\beta$ ,  $\alpha$  and  $\pi^*$

Indicator	$\beta$ / %	$\alpha$ / %	$\pi^*$ / %
EBT	20.28	42.25	37.46
SO	57.98	37.73	4.29
AYR	39.34	16.9	43.76
ATA	32.70	59.05	8.25
AYGG	38.00	12.05	49.95
TY	70.74	1.60	27.66

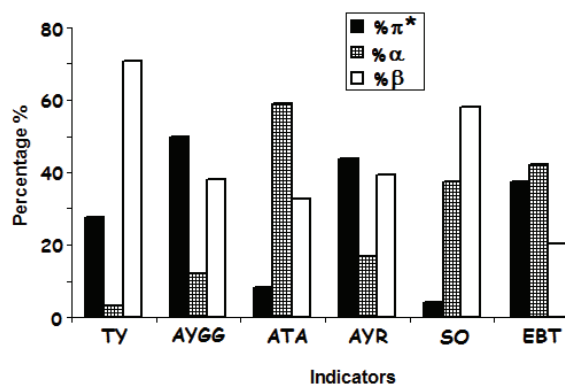


Fig. 4. Percentage contribution of the solvatochromic parameters,  $\pi^*$ ,  $\alpha$  and  $\beta$ .

From Table III, the solvatochromic shifts which arise from the hydrogen bond donating ability ( $\alpha$ ) of the solvents are greater than the  $\pi^*$  and  $\beta$  values in the case of ATA. This could be explained by the interaction of the hydrogen

bonding donating solvents with the carbonyl group of the three carboxylic groups of the benzene rings. However, EBT showed less HBD ability, ( $\alpha = 42.25\%$ ), compared to that observed for ATA, ( $\alpha = 59.05\%$ ), Table III. These results may be attributed to the presence of one  $\text{NO}_2$  group in the former and three carboxy groups in the latter, beside the fact that  $\text{NO}_2$  has less hydrogen bond strength than the carboxylic group.<sup>23</sup> The greater contribution of the HBA ability ( $\beta$  term) on the solvatochromism for SO suggests the existence of the OH–solvent interaction. For TY, the effect of HBD ability ( $\alpha$ ) on the bathochromic shift is practically negligible, contrary to which, the  $\beta$  coefficient has a significant value, and this may be explained by the existence of two sulfonic groups together with the NH group.

*Effect of pH on the electronic absorption spectra of the studied indicators*

The electronic absorption spectra of the indicators under investigation at different pH values indicated that the intensity and the band position are pH dependent with the presence of some isobestic points, Fig. S-2 of the Supplementary material. The isobestic point had been taken as a proof of the existence of an equilibrium between two absorbing species. The electronic spectral data at different pH values are used to compute the dissociation constant of the indicators. Three different spectrophotometric methods are applied to calculate the  $\text{p}K_a$  values. The half-height,<sup>24</sup> the modified limiting absorption,<sup>25</sup> and Colleter<sup>26</sup> methods – as modified for acid base equilibrium<sup>27</sup> – gave reliable results (Table IV and Fig. 5). Different positions are available for protonation (e.g.,  $-\text{N}=\text{N}-$  to give  $\text{H}-\text{N}^+=\text{N}-$ ). The azo-hydrazone tautomerism can be strongly influenced by the synergetic tautomerism in another portion of the molecule.<sup>28</sup>

TABLE IV.  $\text{p}K_a$  values of the compounds (0.5 M KCl, 20 °C)

Compound	Average $\text{p}K$		Colleter		Modified limiting absorption		Half height		$\lambda / \text{nm}$
	$\text{p}K_2$	$\text{p}K_1$	$\text{p}K_2$	$\text{p}K_1$	$\text{p}K_2$	$\text{p}K_1$	$\text{p}K_2$	$\text{p}K_1$	
EBT	9.76±0.04	6.60±0.10	9.79	6.50	9.78	–	9.70	6.70	539
SO	9.51±0.07	5.71±0.14	9.57	5.94	9.45	5.60	9.50	5.60	521
AYGG	–	–	–	–	–	–	–	11.5	259
	–	11.1±0.47	–	10.4	–	11.4	–	11.5	350
ATA	–	–	–	–	–	–	–	4.80	305
	9.48±0.06	4.48±0.22	9.55	4.46	9.40	4.17	9.50	4.80	224
AYR	–	11.13±0.35	–	10.6	–	–	11.28	–	480

Sudan orange (SO) or 1-phenylazo-2-naphthol is a monoprotic dye.<sup>1</sup> It belongs to the azo compounds and has different possible structures in solutions. Under acidic conditions, the azo group could be protonated from the medium giving the azonium form of SO, [I]. The neutral SO can exist in azo–hydrazone equilibrium, [II]. Where in alkaline solutions, SO exist as an anion, [III], Scheme 1.



The calculations at 521 nm using the three mentioned spectrophotometric methods reveal two  $pK_a$  values,  $5.71 \pm 0.14$  and  $9.51 \pm 0.07$ .

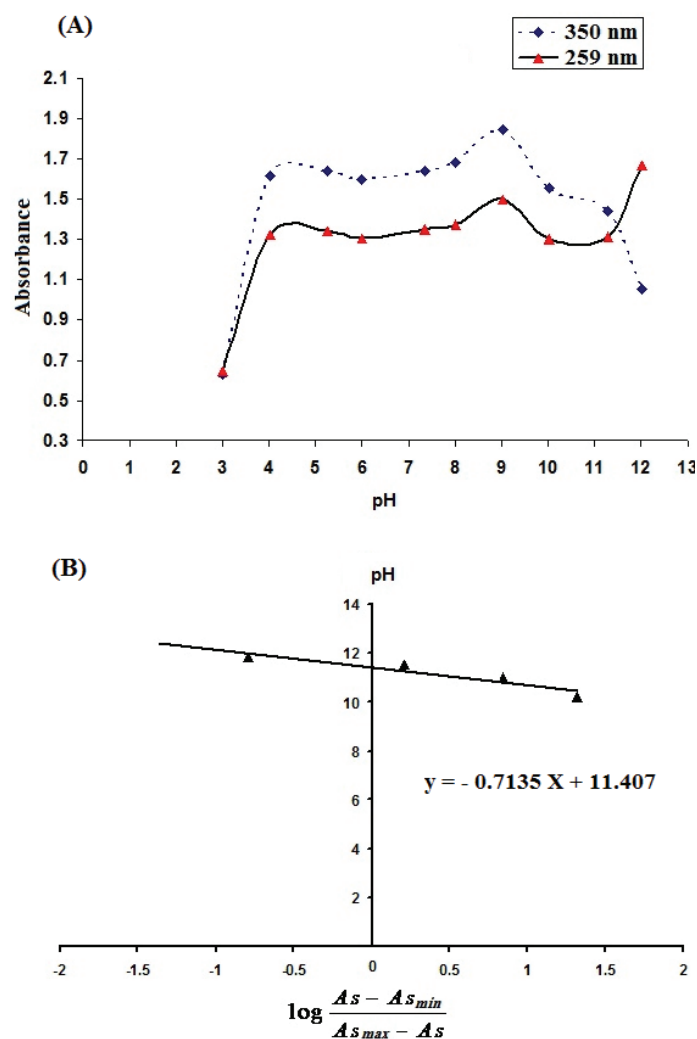
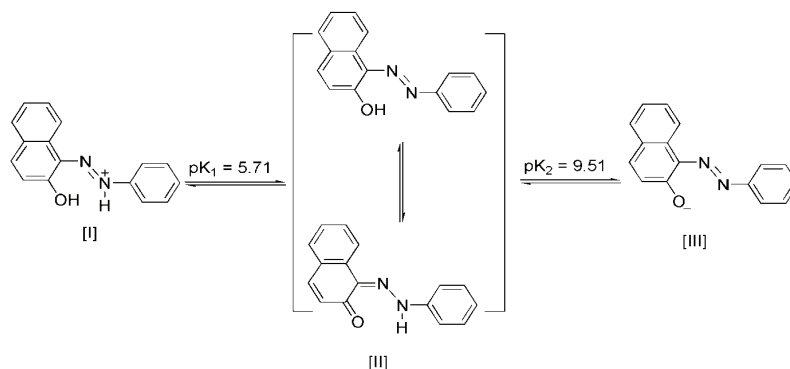


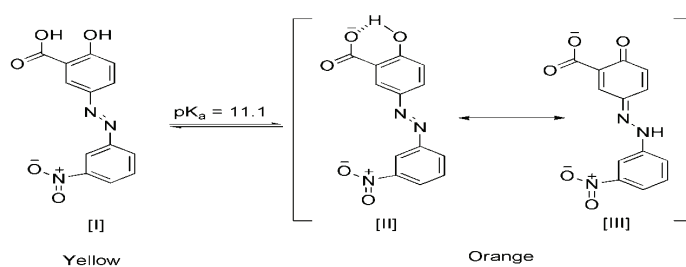
Fig. 5. A) The half height method; absorbance *versus* pH curve of AYGG at two different wavelengths ( $pK_a$  11.5), B) modified limiting absorption method, log of absorbance ratio *versus* pH of AYGG at  $\lambda = 350$  nm.

AYGG is an acid-base indicator with a dye content of 50 %. Its colour is yellow at pH 10 and it changes to orange at pH 12.<sup>1</sup> The electronic spectra of  $1 \times 10^{-4}$  M solution of AYGG in (50 vol. % ethanol–water solution) showed two well-defined bands centred at 275 nm ( $\pi-\pi^*$ ), and at 380 nm ( $n-\pi^*$  of OH group),



Scheme 1. Cationic (I), neutral (II) and anionic (III) of SO in equilibrium with changing of pH.

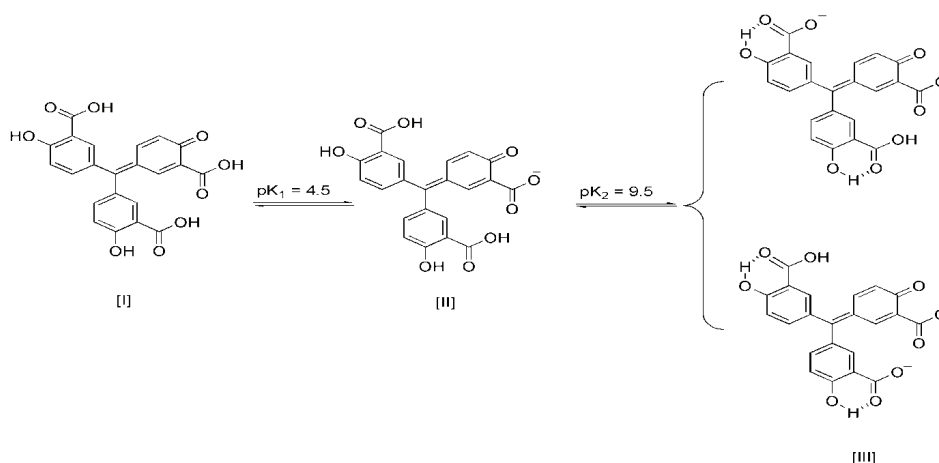
Fig. S-2. For solutions of  $\text{pH} \leq 10$ , these two absorption bands increase stepwise in intensity, with no change in position. However, these two bands are lowered in intensity and a third broad band centered at 480 nm appeared at  $\text{pH} \geq 11$ . This new band displays the formation of the hydrazone form of AYG G [III] as in Scheme 2. Calculations at 350 nm reveal only one  $\text{pK}_a$ , namely  $\text{pK}_1 11.1 \pm 0.47$ , Table IV, which is attributed to the dissociation of the carboxylic acid group, [I]. The electron-donating OH group in the ortho position decreased the acidity of the carboxylic group and therefore lead it to ionize at pH higher than expected ( $\text{pK}_a 11.1$ ). AYG G is a diprotic indicator, however, the  $\text{pK}_2$  value related to *o*-OH group is difficult to be recorded (beyond the pH range of the present study). An explanation for this difficulty is the formation of the hydrazone, [III], and the formation of the intramolecular hydrogen bond between the OH group and the  $\text{COO}^-$  group, [II], that decreases the ionization of the OH group.



Scheme 2. Dissociation pattern of the carboxylic acid group of AYG G.

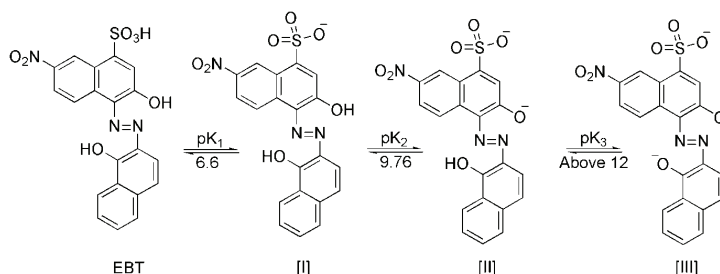
AYR has the same chemical structure as that of AYG G except that the nitro group is in the para position to the azo link, whereas it is in the meta position in the AYG G (Fig. S-1). Despite of this difference the  $\text{pK}_a$  of AYR ( $11.13 \pm 0.35$ ), Table IV, is more or less the same value obtained in the case of AYG G and a similar dissociation pattern for AYR is expected as in Scheme 2.

ATA is a chemical compound that readily polymerizes in aqueous solution.<sup>1</sup> Similar to AYGG, a third band centered at 360 nm appeared in the solution of ATA at  $\text{pH} \geq 11$ . This could be taken as an evidence for the ionization of the OH groups of ATA. Calculations at 305 nm reveal two  $\text{pK}_a$  values,  $\text{pK}_1 4.48 \pm 0.22$  and  $\text{pK}_2 9.48 \pm 0.06$ .  $\text{pK}_1$  is attributed to the dissociation of the carboxylic acid group which is in the *ortho* position to the keto group, [I], Scheme 3. The electron-withdrawing keto-group in this position increases the acidity of the carboxylic group and lead it to ionize at low pH. Whereas,  $\text{pK}_2$  represents the ionization of one of the remaining carboxylic acid groups, [II], Scheme 3. The calculated number of ionized protons for the latter step was found to be around 0.5, indicating that this step has two different paths and suggesting that the two carboxylic acid groups are not equivalent. The ionization of the OH groups of ATA may take place at pH greater than 12, beyond our study range.



Scheme 3. Suggested dissociation pattern of ATA.

EBT is a triprotic dye, in aqueous solutions, the ( $-\text{SO}_3\text{H}$ ) proton is completely dissociated, [I], Scheme 4. The dissociation of the two hydroxyl groups of EBT takes place depending upon pH values. Calculations at 530 nm reveal only



Scheme 4. Suggested dissociation pattern of EBT.

two  $pK_a$  values,  $6.6 \pm 0.01$  and  $9.76 \pm 0.04$ . The  $pK_1$  value of 6.6 is attributed to the dissociation of the sulfonic group of the neutral form of EBT. However, the  $pK_2$  value of 9.76 is attributed to the dissociation of the OH group of the nitro-substituted naphthalene moiety, as the electron-attracting nitro and sulfonic groups lower the  $pK_a$  value. The  $pK_a$  value of the OH group of the naphthalene moiety could not be detected in our study, which suggests that its value could be above 12.<sup>29</sup>

#### *Distribution of species of AYR and SO at different pH values*

In the distribution diagrams, a plot of the fraction of an acid species versus how that fraction varies with pH was made (Fig. 6). The variation of the species is due to the acid dissociation, shifting as pH changes. From these diagrams, the prevailing acid species (undissociated acid or any acid anion) at any pH range could be judged. It is of interest to note that in many cases an intermediate acid anion can never be found as an only species at any pH range. For AYR, HA (undissociated acid species, Fig. 6A), exists predominately below pH 9.1 and it is also in equilibrium with its anion form  $A^-$ , as proved from the electronic spectra. For SO (HA), the  $pK_1$  at 5.71, Table IV, could be explained by the protonation of SO under acidic condition forming  $H_2A^+$  (Fig. 6B). The  $pK_2$  equals 9.51 where  $A^-$  is formed by the ionization of the OH group and reaches its maximum at pH around 11.2.

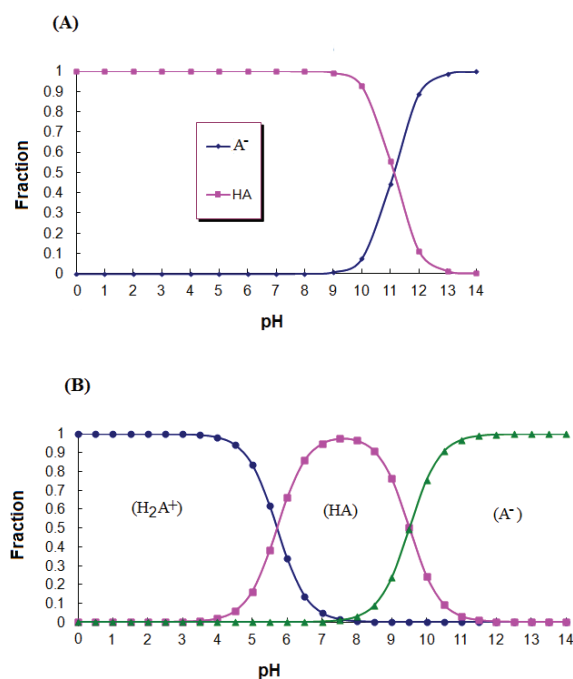


Fig. 6. Distribution diagram of the acid species of: A) AYR and B) SO indicators at different pH.

## CONCLUSIONS

The electronic spectra of six indicators, namely Sudan orange, Alizarin yellow R, Aurin tricarboxylic acid, Alizarin yellow GG, Titan yellow and Eriochrome black-T are affected by the nature of the solvents that differ in their properties. This effect can be expressed quantitatively by applying different models: mainly multiple regression and Kamlet-Taft equations. The observed solvatochromism was found to depend on the presence of donor and acceptor substituents in the conjugated systems of the indicator and the physical properties of the solvent molecules. The series of molecules studied here seem to exist in the *trans*-azo isomer with possible azo-hydrazone tautomerism. The pH effects on the wavenumbers of the absorption band maxima of some indicators with different constituents were discussed at room temperature and the mechanism of ionization was explained. The dissociation constants ( $pK_a$ ) of the investigated indicators were precisely assessed – by the methods described in this work – for the first time that is contrary to the literature data, where wide ranges of pH are given for their colour change.

## SUPPLEMENTARY MATERIAL

The chemical structure of the studied indicators, along with their abbreviations, the physical parameters for the solvents, tables containing regression data and the effect of pH spectra are available at the pages of journal website: <http://www.shd.org.rs/JSCS/>, or from the corresponding author on request.

*Acknowledgement.* The authors express appreciation to the Alexandria University, Egypt, for supporting this investigation.

## ИЗВОД

## УТИЦАЈ РАСТВОРАЧА, СУПСТИТУЕНАТА И рН НА СПЕКТРАЛНЕ ПОМЕРАЈЕ НЕКИХ ВЕОМА ОБОЈЕНИХ ИНДИКАТОРА

MAMDOUH S. MASOUD, REHAB M. I. ELSAMRA и SOKAINA S. HEMDAN

*Department of Chemistry, Faculty of Science, Alexandria University, Alexandria, Egypt*

Солватохромни ефекат шест индикатора, суданско нараџасто, ализарин жуто R, аурин-трикарбоксилна киселина, ализарин жуто GG, титанско жуто и ериохром црно-T, растворених у седам растварача различите поларности, испитиван је на собној температури. Помераји у UV/Vis апсорпционим спектрима су анализирани вишеструком линеарном регресионом анализом и применом Камлет-Тафтове једначине. Нађено је да детектовани солватохромизам зависи од присуства донорских и акцепторских супституената у конјугованим системима индикатора и физичких својстава молекула растварача. Утицај рН на положај максимума апсорпционе траке неких индикатора са различитим супституентима на собној температури је дискутован и објашњен је механизам јонизације. Константе дисоцијације ( $pK_a$ ) испитиваних једињења прецизно су одређене и постојање појединачних доминантних јонских врста је потврђено конструисањем дијаграма расподеле у различитим опсезима рН вредности.

(Примљено 4. фебруара, прихваћено 2. марта 2017)

## REFERENCES

1. R. W. Sabnis, *Hand book of acid-base indicators*, Squire, Sanders & Dempsey LLP, San Francisco, CA, 2007
2. M. S. Zakerhamidi, M. Keshavarz, H. Tajalli, A. Ghanadzadeh, S. Ahmadi, M. Moghadam, S. H. Hosseini, V. Hooshangi, *J. Mol. Liquids* **154** (2010) 94
3. G. S. Uscumlic, J. B. Nikolic, *J. Serb. Chem. Soc.* **74** (2009) 1335
4. Y. D. Daldal, E. C. Demiralay, S. A. Ozkan, *J. Braz. Chem. Soc.* **27** (2016) 493
5. M. S. Masoud, A. M. Hindawy, M. A. Mostafa, A. M. Ramadan, *Spectrosc. Lett.* **30** (1997) 1227
6. M. S. Masoud, E. A. Khalil, A. M. Ramadan, Y. M. Gohar, A. H. Sweyllam, *Spectrochim. Acta, A* **67** (2007) 669
7. M. S. Masoud, E. A. Khalil, A. M. Ramadan, S. A. Mokhtar, O. F. Hafez, *Syn. React. Inorg. Metal-Org. Nano-Metal Chem.* **44** (2014) 402
8. M. S. Masoud, A. M. Hafez, M. Sh. Ramadan, A. E. Ali, *J. Serb. Chem. Soc.* **67** (2002) 833
9. M. S. Masoud, A. M. Hindawy, A. A. Soayed, M. Y. Abd El-Kaway, *Fluid Phase Equilib.* **312** (2011) 37
10. M. S. Masoud, E. A. Khalil, S. Abou El Enein, H. M. Kamel, *Eur. J. Chem.* **2** (2011) 420
11. M. S. Masoud, A. M. Ramadan, A. A. Soayed, S. M. S. Ammar, *J. Iranian Chem. Soc.* **13** (2016) 931
12. F. W. Fowler, A. R. Katritzky, R. J. D. Rutherford, *J. Chem. Soc., B* (1971) 460
13. C. Reichardt, *Chem. Rev.* **94** (1994) 2319
14. J. G. Kirkwood, *J. Chem. Phys.* **2** (1934) 351
15. J. G. David, H. E. Hallam, *Spectrochim. Acta, A* **23** (1967) 593
16. M. J. Kamlet, J.-L. M. Abboud, M. H. Abraham, R. W. Taft, *J. Org. Chem.* **48** (1983) 2877
17. L. J. Hilliard, D. S. Foulk, H. S. Gold, C. E. Rechsteiner, *Anal. Chim. Acta* **133** (1981) 319
18. R. W. Taft, J.-L. M. Abboud, M. J. Kamlet, *J. Org. Chem.* **49** (1984) 2001
19. M. Dakiky, K. Kanan, K. Khamis, *Dyes Pigm.* **41** (1999) 199
20. İ. Sıdır, E. Taşal, Y. Gülseven, T. Gungor, H. Berber, C. Oğretir, *Int. J. Hydrogen Energy* **34** (2009) 5267
21. N. M. Rageh, *Spectrochim. Acta, A* **60** (2004) 103
22. A. R. Monahan, A. F. De Luca, A. T. Ward, *J. Org. Chem.* **36** (1971) 3838
23. N. Valentic, D. Mijin, G. Uscumlic, A. Marinkovic, S. Petrovic, *Arkivoc* **12** (2006) 81
24. R. M. Issa, H. Sadek, I. I. Ezzat, *Z. Phys. Chem.* **74** (1971) 17
25. A. A. Muk, M. B. Pravica, *Anal. Chim. Acta* **45** (1969) 534
26. J. C. Colleter, *Ann. Chim. (Paris)* **5** (1960) 415
27. D. V. Jahagirdar, D. D. Khanolkar, *J. Inorg. Nucl. Chem.* **35** (1973) 921
28. P. W. Alexander, R. J. Sleet, *Aust. J. Chem.* **23** (1970) 1183
29. E. Bosch, J. Guiteras, A. Izquierdo, M. D. Prat, *Anal. Lett.* **21** (1988) 1273.